Hindawi
Advances in Polymer Technology
Volume 2020, Article ID 2914375, 7 pages
https://doi.org/10.1155/2020/2914375

Research Article

Study on Wellbore Temperature and Pressure Distribution in Process of Gas Hydrate Mined by Polymer Additive CO_2 Jet

Minghui Wei, Chenghuai Wu, and Yanxi Zhou

College of Mechanical and Electrical Engineering, Southwest Petroleum University, Chengdu, China

Correspondence should be addressed to Minghui Wei; wmh881988@163.com

Received 29 May 2019; Revised 24 July 2019; Accepted 31 July 2019; Published 10 January 2020

Guest Editor: Hou Jian

In order to solve the problem of hydrate reservoir collapse and hydrate regenerated in the process of solid fluidization of natural gas hydrate, a new method of natural gas hydrate exploit by high-polymer additive (low viscosity carboxymethyl cellulose LV-CMC) carbon dioxide jet was proposed. The wellbore temperature and pressure changes during this process are analyzed, and the wellbore temperature and pressure model are established and solved by the state space method. This paper also analyzed the effects of relevant parameters on hydrate decomposition, such as injection flow, temperature, and pressure. The results show that increasing the injection pressure allows the hydrate decomposition site to be closer to the annulus outlet. Compared with water, with polymer additive CO_2 fluid as the drilling fluid, the intersection point of phase equilibrium curve and annular pressure curve is closer to annular outlet, which is obviously more conducive to well control. In order to avoid phase changes, the injection pressure of the carbon dioxide fluid of the high-polymer additive should not be lower than 10 MPa, and the injection temperature should not be higher than 285 K.

1. Introduction

Natural gas hydrate has great potential for future energy resources supply, which has the characteristics of wide distribution, shallow burial, and high energy density. According to the conditions of temperature less than 283 K and the pressure greater than 10 MPa, about 27% of the world's land and 90% of the ocean have the potential for gas hydrate formation generation. The reserves of natural gas hydrates in the world are very large. It is estimated that the natural gas resources in hydrates are 2×10^{16} m^3, which is equivalent to 2×10^5 billion tons of oil equivalent, and twice the total amount of carbon of conventional fuels in the world. Traditional gas hydrate mining methods include heat injection method, decompression method, carbon dioxide replacement method, etc., But these methods have not been widely used because of the problems of wellbore safety, production control, and environmental risk [1–3]. The natural gas hydrate solid fluidized mining method could overcome these problems effectively [4]. The method is to use the jet to break the bottom hole hydrate into fine particles, and the hydrate-containing solid particles after fluidization return along the wellbore to the sea surface with the drilling fluid, and finally separate out the natural gas.

In the natural gas hydrate solid fluidized mining method, the hydrate reservoir is liable to collapse, and the decomposed natural gas hydrate may be regenerated, causing blockage of the wellbore and causing a drilling accident [5]. Carbon dioxide fluid containing LV-CMC as jet drilling fluid can effectively solve these problems, on the one hand, because both carbon dioxide and LV-CMC can inhibit the formation of natural gas hydrate; on the other hand, LV-CMC, as a drilling fluid additive, also plays a role in reducing leakage and preventing collapse. In addition, in order to prevent the jet viscosity from being too large and affecting the jet efficiency, we use a jet drilling fluid with an additive concentration of 5%. And when the concentration of the polymer additive is 5%, the physical properties of the carbon dioxide fluid are not greatly affected [6].

Carbon capture and storage (CCS) is a technology that can reduce carbon emissions from fossil fuels on a large scale [7]. The technology was developed in the 1970s for oil, geothermal and other energy development, as well as water treatment and other technologies [8–15]. In the process of extracting natural gas hydrates using high-polymer additive carbon dioxide jet, correct prediction of wellbore temperature and pressure is of great significance for judging the properties of polymer additive CO_2 fluid and analyzing the state of

natural gas hydrate. However, there is very little research work in this field.

Since 1950s, drilling workers have begun to study the temperature distribution of wellbore by numerical simulation and analytical method [15]. The earliest wellbore temperature study was conducted by Ramey, who proposed a steady-state model for obtaining wellbore temperature distribution, which could not be applied to transient behavior [16–19]. Raymond proposed a numerical model for wellbore temperature distribution under pseudo-steady-state conditions [20]. Hansan and Kabir proposed an analytical method for wellbore temperature prediction [21, 22]. For CO_2 injection drilling and development methods, wellbore flow and thermal behavior have unique characteristics. Many researchers also developed CO_2 two-phase flow models under isothermal conditions [23–24]. However, the process of natural gas hydrate exploitation is different from injecting polymer additive CO_2 fluid into wellbore. It also needs to consider the heat transfer of annular, pipeline, seawater, and hydrate decomposition, but this field has not been studied for the time being.

In this paper, the mathematical model of wellbore temperature and pressure during polymer additive CO_2 fluid injection is established, and the model is solved by state space method. This method can be used not only to solve partial differential equations, but also as an automatic control model, which lays a foundation for automatic control of temperature and pressure in natural gas hydrate mining process in the future. This study can be used to design the injection parameters of polymer additive CO_2 fluid and reduce the risk of using this drilling fluid to extract natural gas hydrate.

2. Materials and Methods

Low viscosity carboxymethyl cellulose (LV-CMC) is a polymer. Hydroxyl OH and ether oxygen group on the macromolecular chain are absorbed to the surface of the hydrate crystal. The polymer forces the hydrate crystal to grow around the polymer with a small radius of curvature, thus reducing the rate of hydrate formation and prolonging the time of hydrate crystal nucleus formation. In view of the fact that fluidized natural gas hydrates may be formed again during deep-water oil and gas drilling, we chose carbon dioxide fluid with LV-CMC as jet drilling fluid.

The change of phase state of CO_2 at certain temperature and pressure will lead to change in the properties of carbon dioxide. Figure 1 describes phase change of CO_2, when CO_2 approaches the supercritical state (31.1°C, 7.38 MPa), which is likely to occur somewhere along the wellbore.

2.1. Thermodynamic Properties. In 1996, Span and Wagne [26] proposed a special equation of state for carbon dioxide (hereinafter referred to as the S-W equation). It can be applied to a wide range of applications (216.59 K < T < 1100 K, 0.52 MPa < p < 800 MPa) with high accuracy. Therefore, it is more suitable to calculate the thermodynamic properties of polymer additive carbon dioxide fluid under high temperature and high pressure.

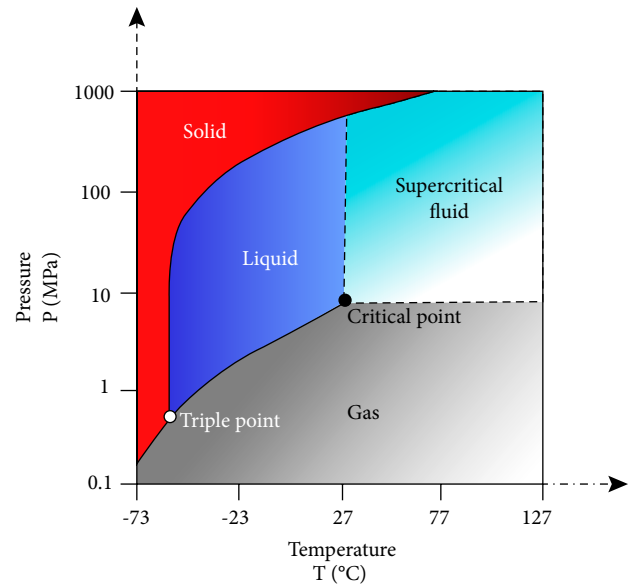

Figure 1: Phase change of carbon dioxide.

The S-W equation is expressed in the form of Helmholtz free energy with two independent variable temperatures T and density ρ. The dimensionless Helmholtz free energy $\Phi(\delta, \tau)$ can be divided into the ideal gas part $\Phi^0(\delta, \tau)$ and the residual fluid part$\Phi^t(\delta, \tau)$, namely:

$$\Phi(\delta, \tau) = \Phi^0(\delta, \tau) + \Phi^t(\delta, \tau) \tag{1}$$

here $\delta = \rho_c/\rho$, $\tau = T_c/T$, dimensionless.

According to the S-W formula and proportion of additive (5%), the solution of the density, isostatic heat capacity, Joule-Thomson coefficient and other thermodynamic properties of the polymer additive CO_2 fluid can be obtained.

2.2. Heat Transfer Model. Figure 2 describes the process of injecting the polymer additive CO_2 fluid for natural gas hydrate exploitation. The process can be divided into three parts. The first, the polymer additive CO_2 fluid is injected into the coiled tubing. The second, the fluids flow through the jet bit and flow into the annulus. The third, the fluids flow through the annulus and to the sea surface.

Based on the principle of conservation of energy, we can establish the dynamic mathematical model of heat transfer in the process of injecting the polymer additive CO_2 fluid:

2.2.1. The heat transfer model of tubing fluids. For the polymer additive CO_2 fluid in the tubing, the energy change is equal to the heat generated by the axial flow of the fluid, the heat exchange between the fluid in the tubing and the fluid in the annulus, and the heat generated by the pressure change. Therefore, the heat transfer model is:

$$\rho_b A_p C_p \frac{\partial T_p}{\partial t} = -M_p C_p \frac{\partial T_p}{\partial z} + 2\pi r_1 \lambda_{12}\left[T_w - T_p\right] + \alpha_p M_p C_p \frac{\partial p_p}{\partial z}, \tag{2}$$

where ρ_b is the density of tubing fluid, kg/m^3, A_p is the area of the tubing, m, T_p is the temperature of the fluid in the tubing,

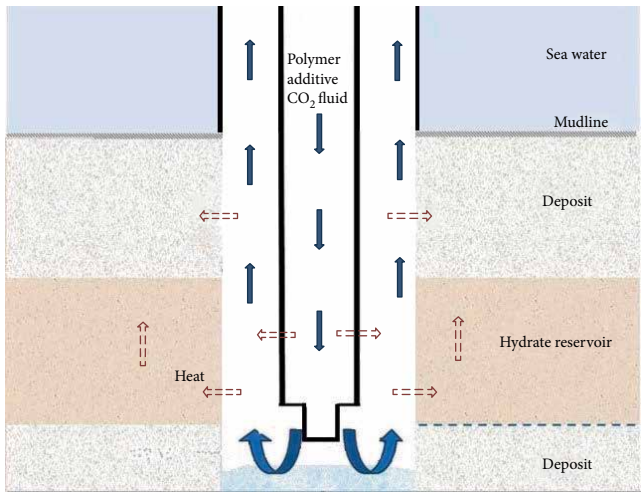

FIGURE 2: Schematic diagram of polymer additive CO_2 fluid injection process.

K, T_w is the temperature of the tubing, K, p_p is the pressure of the fluid in the tubing, MPa, C_p is the specific heat of tubing fluids, J/kg·K, r_1 is the inner radius of tubing, m, v_p is the fluids flow velocity in the tubing, m/s, λ_{12} is the convective heat transfer coefficient between tubing the polymer additive CO_2 fluids and tubing, W/m^2·K, and α_p is Joule-Thomson coefficient, K/MPa.

2.2.2. The heat transfer model of annulus. According to Figure 2, we can know the heat transfer model of the polymer additive CO_2 fluid in the annulus. The energy change is equal to the heat generated by the axial flow of the fluid, the heat transfer between the annulus fluid and the pipeline fluid, and the heat transfer between the wellbore fluid and the annulus fluid. Therefore, the heat transfer model is:

$$\begin{aligned}\rho_a A_a C_a \frac{\partial T_a}{\partial t} = &- M_a C_a \frac{\partial T_a}{\partial z} + 2\pi r_2 \lambda_2 [T_w - T_a] \\ &+ 2\pi r_3 \lambda_3 \left[T_f - T_a\right] + \alpha_a M_a C_a \frac{\partial p_a}{\partial z},\end{aligned} \tag{3}$$

where ρ_a is the polymer additive CO_2 fluid density of annulus, kg/m^3, A_a is the area of annulus, m^2, T_a is the temperature of the fluid in the annulus, K, T_w is the temperature of the tubing, K, p_a is the pressure of the fluid in the annulus, MPa, C_a is the polymer additive CO_2 fluid specific heat of annulus fluid, J/kg·K, M_a is the mass flow of injected polymer additive CO_2 fluid, kg/s, r_2 is the outer radius of tubing, m, r_3 is the radius of annulus, m, λ_{21} is the convection heat transfer coefficient of annular fluid and tubing, λ_3 is the convection heat transfer coefficient of annular fluid and borehole wall, W/m^2·°C, α_a is the Joule-Thomson coefficient, K/MPa.

2.2.3. The heat transfer model of tubing. For the tubing, the change of energy is equal to the convection heat transfer between the annulus fluids and tubing, and the convection heat transfer between the tubing fluids and tubing. Therefore, the heat transfer model is:

$$\rho_w A_w C_w \frac{\partial T_w}{\partial t} = 2\pi r_2 \lambda_{21} [T_a - T_w] + 2\pi r_1 \lambda_{12} \left[T_p - T_w\right], \tag{4}$$

where ρ_w is the density of tubing, kg/m^3, A_w is the area of tubing, m^2, and C_w is the specific heat of tubing, J/kg·K.

2.3. Wellbore Pressure Model. According to the mass conservation equation and momentum equation, we can get the wellbore pressure model:

$$\frac{\partial}{\partial z}(p_a v_a) = 0 \tag{5}$$

$$\frac{\partial}{\partial z}\left(p_a {v_a}^2\right) = -\frac{\partial p_a}{\partial z} + \rho_a g \sin\theta - \frac{\tau_w \pi d}{A_p}. \tag{6}$$

Substituting the mass conservation equation into the momentum equation and replacing the friction term of wall, flowing pressure equation of the polymer additive CO_2 fluid flow downward in the tubing can be deduced

$$\frac{\partial p_a}{\partial z} = -\rho_a g \frac{\partial v_a}{\partial z} + \rho_a g \sin\theta - f \frac{\rho v_a^2}{2d}, \tag{7}$$

where f is Darcy friction factor and v_a is annulus flow rate, m/s.

2.4. Hydrates Phase Equilibrium Model. According to Dzyuba's natural gas hydrate phase equilibrium model [4], the relationship between temperature and pressure is:

$$p_E = \frac{T_a - 264.9661}{9.6339}, \tag{8}$$

where p_E is hydrate phase equilibrium pressure at the temperature T_a, MPa.

2.5. State-Space Method for the Wellbore. For Equation (4), using difference instead of integral, therefore:

$$\begin{aligned}\frac{\partial T}{\partial t} &= \frac{T(k+1,1) - T(k,1)}{\Delta t}, \\ \frac{\partial T}{\partial z} &= \frac{T(1,j) - T(1,j-1)}{\Delta z}.\end{aligned} \tag{9}$$

Equation (2) can be expressed as:

$$\begin{aligned}\rho_a A_a C_a \frac{T_a(k+1,j) - T_a(k,j)}{\Delta t} = &- M_a C_a \frac{T_a(k,j) - T_a(k,j-1)}{\Delta z} \\ &+ 2\pi r_2 \lambda_2 [T_w(k,j) - T_a(k,j)] \\ &+ 2\pi r_3 \lambda_3 \left[T_f(k,j) - T_a(k,j)\right] \\ &+ \alpha_a M_a C_a \frac{\partial p_a}{\partial z}.\end{aligned} \tag{10}$$

The depth of wellbore is divided into L nodes, according to linear system theory, each grid temperature in the tubing and annulus is a state. We set the gas injection temperature as $T_a(k,0)$, and set $x_1 = -(M_a \Delta t)/(\rho_a A_a \Delta z)$, $x_2 = 2\pi r_2 \lambda_2 \Delta t/(\rho_a A_a C_a)$, $x_3 = 2\pi r_3 \lambda_3 \Delta t/(\rho_a A_a C_a)$, $Q = \alpha_a M_a C_a (\partial p_a)/(\partial z)$, the state-space model for wellbore heat transfer system can be represented as:

$$T_A(k+1) = A_a T_A(k) + B_a T_w(k) + C_a T_f(k) + D_a U_d(k), \tag{11}$$

where,

$$T_A(k) = \left[T_a(k,1), T_a(k,2), T_a(k,3), \cdots T_a(k,L)\right]^T_{L\times 1} \tag{12}$$

$$T_w(k) = \left[T_w(k,1), T_w(k,2), T_w(k,3), \cdots T_w(k,L)\right]^T_{L\times 1} \tag{13}$$

$$T_f(k) = \left[T_f(k,1), T_f(k,2), T_f(k,3), \cdots T_f(k,L)\right]^T_{L\times 1} \tag{14}$$

$$U_d(k) = \left[T_a(k,0), Q, 0, \cdots 0\right]^T_{L\times 1} \tag{15}$$

$$A_a = \begin{bmatrix} x_1+1-x_2-x_3 & 0 & 0 & \cdots & 0 \\ -x_1 & x_1+1-x_2-x_3 & 0 & \cdots & 0 \\ 0 & -x_1 & \ddots & \ddots & 0 \\ \vdots & 0 & \ddots & x_1+1-x_2-x_3 & 0 \\ 0 & 0 & 0 & -x_1 & x_1+1-x_2-x_3 \end{bmatrix}_{L\times L}, \tag{16}$$

$$B_a = x_2,$$
$$C_a = x_3,$$
$$D_a = -x_1,$$

T_A is the state vector of wellbore heat transfer state-space model, U_d is the input vector, and A_a is the system matrix. In the same way, we can get the state space model of the fluid temperature in the tubing.

$$T_P(k+1) = A_p T_P(k) + B_p T_w(k) + D_p U_p(k). \tag{17}$$

In this process, the heat sources are the seawater temperature, the formation temperature and the hydrate reservoir temperature, according to literature [4], we can calculate the seawater temperature

$$T_s = \frac{1}{200}\left[(T_{s0} - 273.15)(200 - z) + 13.7h\right], \quad 0 \le z < 200\,m$$
$$T_s = a_1 - \frac{a_1 - a_2}{1 + e^{z+a_3/a_4}}, \quad z \ge 200\,m, \tag{18}$$

where T_s represents the temperature of seawater, K; T_{s0} represents the temperature of sea surface, K; z represents the depth of seawater, m; a_1, a_2, a_3, a_4 represent curve fitting coefficients, respectively.

3. Results

In order to verify this model, we do simulation to get the distribution of wellbore temperature and pressure and the location of gas hydrate decomposition point under different conditions. The basic data of the simulation derived from literature [4, 23], and are shown in Table 1.

3.1. The Influence of Injection Rate. When the injection rates of the polymer additive CO_2 fluid are 40 L/min, 60 L/min, 80 L/min, and 100 L/min, using this model, the annulus temperature and pressure can be obtained.

Figure 3 shows the temperature distribution of annulus under different polymer additive CO_2 fluid injection rates. The larger the drilling fluid flow rate, the shorter the heat exchange time between the annulus and the seawater, and the less the temperature of annulus is affected by seawater.

Figure 4 shows that annulus pressure decreases as the flow rate increases. For the upper section of wellbore, the phase equilibrium pressure decreases as the flow rate increases, for the lower section of wellbore, the phase equilibrium pressure changes almost unchanged with the change of flow rate. The intersection of annulus pressure and phase equilibrium pressure curve moves upward (The intersection point refers to the critical decomposition position of the natural gas hydrate); this is contrary to the conclusion in [4]. Under this condition of injection temperature and pressure, the decomposition position of hydrate is between depth 150 and 200 m.

During the actual drilling process, phase changes of the polymer additive CO_2 fluid are not expected. According to Figures 4 and 5, the minimum pressure and maximum temperature of the polymer additive CO_2 fluid are at the annulus outlet. The temperature and the pressure corresponding to the different flow rates are shown in Table 2. According to the S-W equation, there is no phase change during this process. In practice, in order to ensure operation safely, the injection pressure should be increased and the injection temperature should be reduced as possible.

3.2. The Influence of Injection Temperature. Figure 5 shows the annulus pressure and phase equilibrium curves under different injection temperatures, when the flow rate is 100 L/min. Due to the injection temperature increase, the phase equilibrium pressure increases, and the annulus pressure increases a little. The injection temperature effects on the depth of decomposition point very little.

Table 1: Calculation parameters.

Parameter	Value	Parameter	Value
Well depth/m	1200	Mass flow rate/(L/min)	40
Coiled Tubing inner diameter/mm	40	Injection pressure/MPa	25
Coiled Tubing outer diameter/mm	51	Injection temperature/°C	21
Drilling string inner diameter/mm	114	Surface earth temperature/°C	20
Drilling string outer diameter/mm	127	Fluids density/(kg/m3)	1040

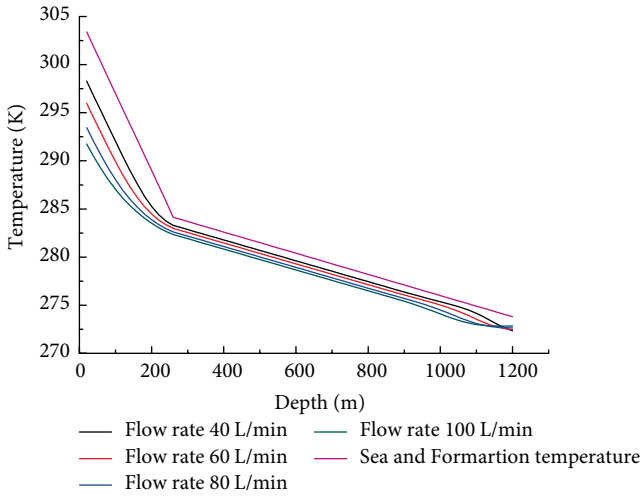

Figure 3: The annulus temperature distribution with different injection rate.

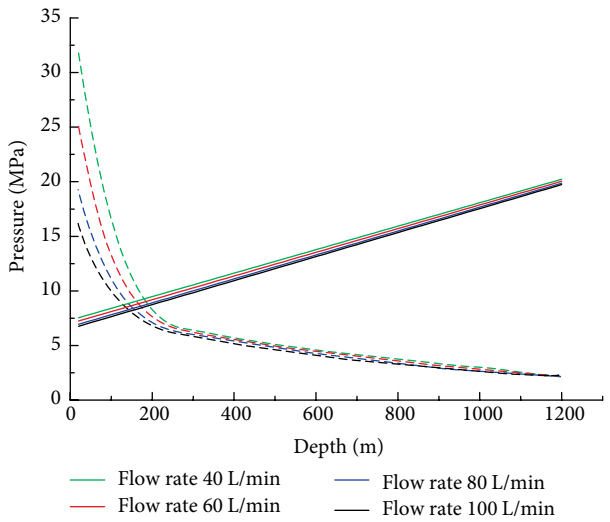

Figure 4: The annulus pressure distribution and hydrates phase equilibrium with different injection rates.

3.3. Comparison With Water. In order to compare the difference between using polymer additive CO_2 fluid and using water as drilling fluid, we do the simulation. As in practice, water is difficult to achieve low temperature as a drilling fluid, the injection water temperature is set at 285 K, the injection pressure is 10 MPa, and the injection amount is 10 L/min. The polymer additive CO_2 fluid injection temperature is 275 K, and other conditions keep the same.

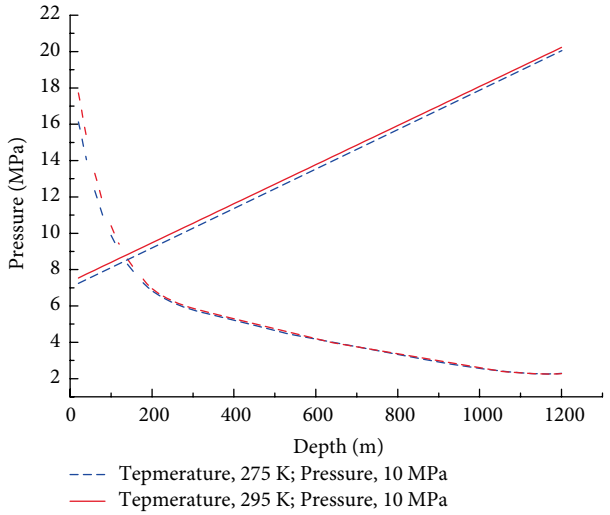

Figure 5: The annulus pressure distribution and hydrate phase equilibrium with different injection temperatures.

Table 2: Flow rate-pressure/temperature.

Flow rate, L/min	Pressure, MPa/Temperature, K
40	7.54/298.27
60	7.24/295.99
80	6.94/293.45
100	6.76/291.75

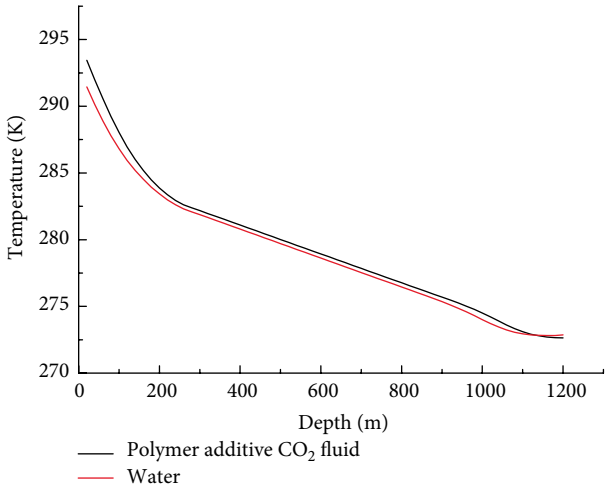

Figure 6: The annulus temperature distribution comparison between the polymer additive CO_2 fluid and water as drilling fluids.

Figure 6 shows the annulus temperature distribution. Since the specific heat of the polymer additive CO_2 fluid is less than the specific heat of the water, it is greatly affected by the seawater

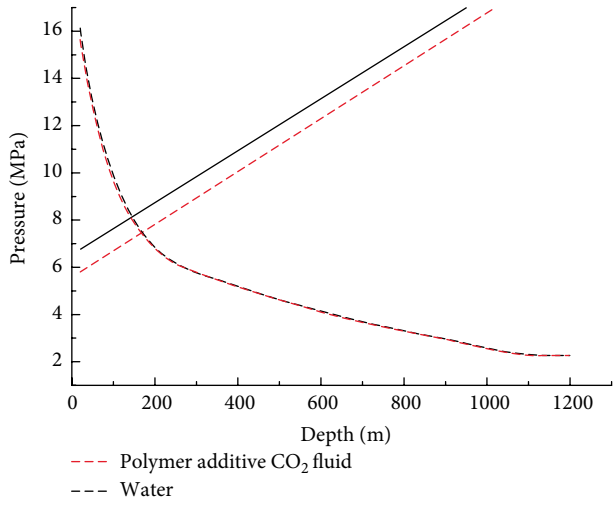

FIGURE 7: The annulus pressure distribution and hydrates phase equilibrium comparison between the polymer additive CO_2 and water as drilling fluids.

temperature. Figure 7 shows the relationship between the annulus pressure and the phase equilibrium pressure. The equilibrium curves of the two are almost coincident. When polymer additive CO_2 fluid is used as the drilling fluid, the decomposition position of the hydrate is closer to the wellhead.

4. Conclusions

Based on the above study, we can draw the following conclusions:

(1) Increasing the pressure of injection can get the hydrate decomposition position closer to the annulus outlet.

(2) Compared with water, using polymer additive CO_2 fluids as drilling fluids, the intersection of phase equilibrium curve and the annulus pressure curve is closer to the annulus outlet, which is obviously beneficial to the implementation of well control.

(3) However, due to the special properties of the polymer additive CO_2 fluid, in order to ensure that the polymer additive CO_2 fluids do not result in a phase change during the drilling process, it is necessary to increase the pressure and reduce the temperature of the injection CO_2; this is very difficult for the equipment. According to the calculation, it is suggested that the injection pressure should not be lower than 10 MPa and the injection temperature should not be higher than 285 K.

(4) When the polymer additive CO_2 fluid is used as the drilling fluid, the intersection of the phase equilibrium curve and the annulus pressure curve increases as flow rate increases, which is contrary to the conclusion in [4]. The reason is the focus of future research.

Data Availability

All data included in this study are available upon request by contact with the corresponding author.

Conflicts of Interest

The authors declare that there is no conflict of interest regarding the publication of this paper.

Acknowledgments

This research was funded by State Key Laboratory of Petroleum Resources and Prospecting, China University of Petroleum, Beijing, grant number PRP/open-1610 and National Natural Science Foundation of China, grant number 51804267.

References

[1] R. C. Zheng, S. H. B. Yang, P. Babu, P. Linga, and X.-S. Li, "Review of natural gas hydrates as an energy resource: prospects and challenges," *Applied Energy*, vol. 162, pp. 1633–1652, 2016.

[2] R. Boswell and T. S. Collett, "Current perspectives on gas hydrate resources," *Energy & Environmental Science*, vol. 4, no. 4, pp. 1206–1215, 2011.

[3] X.-S. Li, B. Yang, Y. Zhang et al., "Experimental investigation into gas production from methane hydrate in sediment by depressurization in a novel pilot-scale hydrate simulator," *Applied Energy*, vol. 93, no. 6, pp. 722–732, 2012.

[4] S. Zhou, Q. Li, W. Chen et al., "The world's first successful implementation of solid fluidization well testing and production for non-diagenetic natural gas hydrate buried in shallow layer in deep water," vol. 4, in *Proceedings of the Annual Offshore Technology Conference*, pp. 2784–2794, Houston, TX, USA, 2018.

[5] L. Zeng, J. Ding, and J. Xu, "Study on a kind of effective compound inhibitor of gas hydrate," *Guangdong Chemical Industry*, vol. 35, no. 3, pp. 8–10, 2008.

[6] B. J. Sun, X. L. Liu, and S. R. Ren, "Experiment on inhibition of drilling fluid additives for natural gas hydrate formation," *Journal of China university of petroleum (Natural Science Edition)*, vol. 32, no. 1, pp. 56–59, 2008.

[7] Z. Chen, X. Liao, X. Zhao, X. Dou, and L. Zhu, "Development of a trilinear-flow model for carbon sequestration in depleted shale," *SPE Journal*, vol. 21, no. 4, pp. 1386–1399, 2016.

[8] T. A. Buscheck, Y. Sun, Y. Hao et al., "Combining brine extraction, desalination, and residual-brine reinjection with CO_2 storage in saline formations: implications for pressure management, capacity, and risk mitigation, Amsterdam Netherlands," *Energy Procedia*, vol. 4, pp. 4283–4290, 2011.

[9] X. Huang, T. Li, H. Gao, J. Zhao, and C. Wang, "Comparison of SO_2 with CO_2 for enhancing shale-hydrocarbon recovery using low-field nuclear magnetic resonance," *Fuel*, vol. 245, pp. 563–569, 2019.

[10] Q. Li, Y. N. Wei, G. Liu, and Q. Liu, "Combination of CO_2 geological storage with deep saline water recovery in western China: insights from numerical analyses," *Applied Energy*, vol. 116, pp. 101–110, 2014.

[11] H. Wang, G. Li, and Z. Shen, "A feasibility analysis on shale gas exploitation with supercritical carbon dioxide," *Energy Sources, Part A: Recovery, Utilization, and Environmental Effects*, vol. 34, no. 15, pp. 1426–1435, 2012.

[12] F. Luo, R.-N. Xu, and P.-X. Jiang, "Numerical investigation of the doublet enhanced geothermal system with CO_2 as working fluid (CO_2-EGS)," *Energy*, vol. 64, pp. 307–322, 2014.

[13] M. Boot-Handford, J. C. Abanades, E. Anthony et al., "Carbon capture and storage update," *Energy Environment Science*, vol. 7, no. 1, pp. 130–189, 2014.

[14] R. S. Middleton, J. W. Carey, R. P. Currier et al., "Shale gas and non-aqueous fracturing fluids: opportunities and challenges for supercritical CO_2," *Applied Energy*, vol. 14, no. 7, pp. 500–509, 2015.

[15] H. Sun, J. Yao, S.-H. Gao, D.-Y. Fan, C.-C. Wang, and Z.-X. Sun, "Numerical study of CO_2 enhanced natural gas recovery and sequestration in shale gas reservoirs," *International Journal of Greenhouse Gas Control*, vol. 19, pp. 406–419, 2013.

[16] A. R. Hasan and C. S. Kabir, "A mechanistic model for computing fluid temperature profiles in gas-lift wells," *SPE Production and Facilities*, vol. 11, no. 3, pp. 179–185, 1996.

[17] H. J. Ramey, "Wellbore heat transmission," *Journal of Petroleum Technology*, vol. 14, no. 4, pp. 427–435, 1962.

[18] M. Yang, X. Zhao, Y. Meng et al., "Determination of transient temperature distribution inside a wellbore considering drill string assembly and casing program," *Applied Thermal Engineering*, vol. 118, pp. 299–314, 2017.

[19] A. R. Hasan and C. S. Kabir, *Fluid Flow and Heat Transfer in Wellbores*, SPE Richardson, Texas, 2002.

[20] L. R. Raymond, "Temperature distribution in a circulating drilling fluid," *Journal of Petroleum Technology*, vol. 21, no. 3, pp. 333–341, 1969.

[21] A. R. Hasan, C. S. Kabir, and X. Wang, "Development and application of a wellbore/reservoir simulator for testing oil wells," *SPE Formation Evaluation*, vol. 12, no. 3, pp. 182–190, 1997.

[22] A. R. Hasan, C. S. Kabir, and X. Wang, "Wellbore two-phase flow and heat transfer during transient testing," *SPE Journal*, vol. 3, no. 2, pp. 174–182, 1998.

[23] H. Wang, Z. Shen, and G. Li, "Influences of formation water invasion on the wellbore temperature and pressure in supercritical CO_2 drilling," *Petroleum Exploration Development*, vol. 38, no. 3, pp. 362–368, 2011.

[24] X. Li, G. Li, H. Wang et al., "A coupled model for predicting flowing temperature and pressure distribution in drilling ultra-short radius radial wells," in *IADC/SPE Asia Pacific Drilling Technology Conference*, Singapore, August 22–24, 2016.

[25] J. Guo and J. Zeng, "A coupling model for wellbore transient temperature and pressure of fracturing with supercritical carbon dioxide," *Shi You Xue Bao/ActaPet. Sin*, vol. 36, no. 2, pp. 203–209, 2015.

[26] R. Span and W. Wagner, "A new equation of state for carbon dioxide covering the fluid region from the triple-toint temperature to 1100 K at pressures up to 800 MPa," *Journal of Physical and Chemical Reference Data*, vol. 25, no. 6, pp. 1509–1596, 1996.

[27] Z. M. Wang, X. N. Hao, X. Q. Wang, L. Xue, and X. L. Guo, "Numerical simulation on deep water drilling wellbore temperature and pressure distribution," *Petroleum Science and Technology*, vol. 28, no. 9, pp. 911–919, 2010.